Preparation and electrochemical properties of high-voltage cathode materials, $LiM_yNi_{0.5-y}Mn_{1.5}O_4$ (M = Fe, Cu, Al, Mg; $y = 0.0$–0.4)

George Ting-Kuo Fey[*], Cheng-Zhang Lu, T. Prem Kumar[1]

Department of Chemical and Materials Engineering, National Central University, Chung-Li 32054, Taiwan, ROC

Abstract

Solid-state synthesized $LiNi_{0.5-y}M_yMn_{1.5}O_4$ spinels, where M = Fe, Mg, Al, or Cu, and $y = 0.0$–0.4, have been studied as high-voltage cathode materials. Powder X-ray diffraction studies showed that all the substituents displayed a propensity for the 8*a* tetrahedral site at high concentrations. Cyclic voltammetric studies showed electrochemical activity around 4 V as well as above 4.4 V. While the 4-V activity was related solely to the Mn^{4+}/Mn^{3+} couple, the 5-V activity was due to the redox reactions of Ni and the other transition metal ions. The co-substituents reduced the 5-V capacity and shifted the redox potentials in the 5-V region to higher values. At high concentrations, the co-substituents tended to occupy the 8*a* sites, which may lead to a blockage of lithium transport during the charge–discharge processes. $LiNi_{0.4}Fe_{0.1}Mn_{1.5}O_4$ registered the best performance with a first-cycle capacity of 117 mAh/g and 78% capacity retention over 60 cycles. Electrochemical impedance spectroscopic studies showed a decrease in the charge transfer resistance at high deintercalation levels.
© 2003 Elsevier Science B.V. All rights reserved.

Keywords: Multiple substitution; Cathode materials; $LiMn_2O_4$; Spinel cathode; Lithium battery

1. Introduction

With a theoretical specific capacity of 148 mAh/g, excellent electrochemical reversibility for the lithium intercalation reaction, good voltage regulation on cycling, low cost and eco-friendliness, $LiMn_2O_4$ qualifies as an attractive cathode material for rechargeable lithium batteries. Although capacities of about 120 mAh/g have been realized even after 100 cycles in the 4-V region [1], the commercial exploitation of $LiMn_2O_4$ has been hampered by its capacity fade upon prolonged cycling especially at elevated temperatures [1–3]. The capacity fade has been attributed to Jahn–Teller distortion [2,4], lattice instability [5,6], manganese dissolution [2–4,7], oxidation of the electrolyte [7,8], formation of oxygen-rich spinels [9], lattice site exchange between lithium and manganese ions [4], and particle disruption [10]. One method adopted to circumvent the poor cyclability of $LiMn_2O_4$ is substituting part of the manganese

with a metal ion that may stabilize the spinel structure of the host compound. Such substitutions can enhance the structural stability of the host structure, although often at the cost of lower 4-V capacity. If the substituent is a transition metal ion like iron, chromium, etc., additional capacity can be tapped at a higher cell voltage. Typically, these substituted spinels are charged and discharged at potentials above 5 V.

Ohzuku et al. [11] studied a series of 5-V cathode materials obtained by substituting Mn in $LiMn_2O_4$ with 3*d* transition metals such as Co, Cr, Cu, Fe, Ni, Ti, and Zn. These materials showed operating voltages above 4.8 V. Lee et al. [12], who studied the degradation mechanism in $LiMn_2O_4$ doped with Li, B, Al, Co, or Ni, showed that volume changes in the spinel during the charging and discharging processes were responsible for the breakdown of the host structure. Recently, Ohzuku et al. [13] reported the formation of a whole series of solid solutions of the general formula $LiFe_yMn_{2-y}O_4$ in iron-substituted systems. They also showed that when the iron content was increased from 0 to 0.5, the 4-V capacity of the spinel decreased while the 5-V capacity increased. The reaction mechanism was studied by Mossbauer spectroscopy [13]. According to Morales et al. [14], iron substitution is believed to result in a disordered structure, which lessens the Jahn–Teller distortion, rendering an improvement in the

[*] Corresponding author. Tel.: +886-3-422-7151-4206/425-7325; fax: +886-3-425-7325.
E-mail address: gfey@cc.ncu.edu.tw (G.T.-K. Fey).
[1] On deputation from: Central Electrochemical Research Institute, Karaikudi 630006, TN, India.

cyclability of the spinel in the 3-V region. Song et al. [15] reported that iron decreased the 4-V capacity, but improved the cycling performance. Copper as a substituent has also been studied [16–19]. The redox processes occurring between 4.8 and 5.0 V has been attributed to the Cu^{3+}/Cu^{2+} couple [18]. The cation distribution in these compounds is complex [18]. Aluminum as a non-transition metal substituent reduced strain in $LiMn_2O_4$ during repeated cycling [12,20] and facilitates higher discharge capacity retention [20]. However, Lee et al. [12] observed a unique effect with aluminum-substituted $LiMn_2O_4$ prepared by a melt-impregnation method: while the substituent led to excellent cycling performance in the 4-V region, it produced an abrupt capacity loss in the 3-V region. The authors [12] attributed this effect to the formation of mixed cubic and tetragonal phases after some initial cycling. Small amounts of magnesium have also been demonstrated to improve cycle performance of the spinel [2,21,22], although the first discharge capacity was considerably lower than the parent $LiMn_2O_4$ [22]. $LiNi_yMn_{2-y}O_4$ materials exhibit electrochemical activity in the 5-V range [23,24]. The higher capacity in the nickel-substituted materials is believed to be due to the oxidation of Ni^{2+} to Ni^{4+} [24]. Nickel-substituted $LiMn_2O_4$ was recently studied as a cathode material in a cell with a Cu–Sn microcomposite anode [25]. The effect of multiple cation substitution in $LiMn_2O_4$ has also been investigated. For example, $LiNi_yCu_{0.5-y}Mn_{1.5}O_4$ was shown to exhibit superior high-potential cathodic properties [11]. Co- and Ni-substituted $LiMn_2O_4$ thin films have also been studied for their electrochemical properties in the 5-V region [26]. Recently, Kawai et al. [27] reviewed high-voltage materials for application in lithium batteries.

This paper reports the effect of cationic substitution in $LiM_yNi_{0.5-y}Mn_{1.5}O_4$ with transition metals (Fe or Cu) or non-transition metals (Mg or Al). The substituent levels were $y = 0.0$, 0.1, 0.2, 0.3, and 0.4. The structural and electrochemical features of the products as lithium-intercalating cathodes are discussed.

2. Experimental

Substituted spinels of the compositions $LiM_yNi_{0.5-y}Mn_{1.5}O_4$ (M = Fe, Mg, Al, or Cu; $y = 0.0$, 0.1, 0.2, 0.3, and 0.4) were synthesized by a solid-state fusion method. Stoichiometric amounts of Li_2CO_3 (Ferax), MnO_2 (Aldrich) and NiO (J.T. Baker), and the respective substituent compound [CuO (Acros), Fe_2O_3 (Ferax), $Al(OH)_3$ (J.T. Baker) or MgO (Acros)] were thoroughly ground in an agate mortar and pelletized. The pellets were then fired in a muffle furnace at 800 °C for 24 h in air. The heating rate was 4.2 °C/min and the cooling rate to room temperature was 3 °C/min. After cooling to room temperature, the pellets were ground again. The chemical compositions of the products were determined by an inductively coupled plasma-mass spectrometer (PE-Sciex Elan Model 6100 DRC), and were found to be close to the targeted formulae (Table 1). It was assumed that the oxidation states of the transition metal ion substituents in the synthesized compounds were 2+, 3+, and 2+ for Ni, Fe, and Cu, respectively. The changes in the local structure of the parent compound because of the substitutions were studied by a Siemens D5000 X-ray diffractometer with nickel-filtered Cu Kα radiation between scattering angles 5° and 80° in increments of 0.05°.

Charge–discharge studies were carried out with coin cells assembled in standard 2032 cell hardware. Lithium metal was used as the anode and a 1 M solution of $LiPF_6$ in EC:DEC (1:1 (v/v)) was used as the electrolyte. The cathode was prepared by blade-coating a slurry of 85 wt.% active

Table 1
Variations in lattice parameters and integrated peak intensity ratios as a function of the dopant concentration in $LiM_yNi_{0.5-y}Mn_{1.5}O_4$ (M = Fe, Mg, Al, Cu; $y = 0.0$–0.4)

System	ICP-MAS analysis	Lattice parameter 'a' (Å)	$I_{(4\,0\,0)}/I_{(3\,1\,1)}$	$I_{(2\,2\,0)}/I_{(3\,1\,1)}$
$LiMn_2O_4$	$Li_{0.970}Mn_{1.982}O_{3.997}$	8.200	1.036	–
$LiNi_{0.5}Mn_{1.5}O_4$	$Li_{0.965}Ni_{0.486}Mn_{1.482}O_{3.933}$	8.145	1.060	–
$LiFe_{0.1}Ni_{0.4}Mn_{1.5}O_4$	$Li_{0.972}Fe_{0.097}Ni_{0.388}Mn_{1.473}O_{3.882}$	8.171	1.072	0.033
$LiFe_{0.2}Ni_{0.3}Mn_{1.5}O_4$	$Li_{0.984}Fe_{0.196}Ni_{0.298}Mn_{1.484}O_{3.925}$	8.173	1.010	0.056
$LiFe_{0.3}Ni_{0.2}Mn_{1.5}O_4$	$Li_{1.002}Fe_{0.297}Ni_{0.201}Mn_{1.470}O_{3.954}$	8.207	0.930	0.080
$LiFe_{0.4}Ni_{0.1}Mn_{1.5}O_4$	$Li_{0.964}Fe_{0.412}Ni_{0.103}Mn_{1.502}O_{3.988}$	8.222	0.927	0.053
$LiMg_{0.1}Ni_{0.4}Mn_{1.5}O_4$	$Li_{0.988}Mg_{0.094}Ni_{0.393}Mn_{1.485}O_{3.947}$	8.166	1.126	0.036
$LiMg_{0.2}Ni_{0.3}Mn_{1.5}O_4$	$Li_{0.978}Mg_{0.193}Ni_{0.291}Mn_{1.479}O_{3.927}$	8.181	1.004	0.045
$LiMg_{0.3}Ni_{0.2}Mn_{1.5}O_4$	$Li_{0.975}Mg_{0.291}Ni_{0.187}Mn_{1.472}O_{3.903}$	8.187	0.987	0.050
$LiMg_{0.4}Ni_{0.1}Mn_{1.5}O_4$	$Li_{0.969}Mg_{0.382}Ni_{0.093}Mn_{1.481}O_{3.912}$	8.194	1.058	0.035
$LiAl_{0.1}Ni_{0.4}Mn_{1.5}O_4$	$Li_{0.978}Al_{0.091}Ni_{0.387}Mn_{1.489}O_{3.936}$	8.175	1.166	0.049
$LiAl_{0.2}Ni_{0.3}Mn_{1.5}O_4$	$Li_{0.973}Al_{0.187}Ni_{0.291}Mn_{1.491}O_{3.937}$	8.153	1.018	0.045
$LiAl_{0.3}Ni_{0.2}Mn_{1.5}O_4$	$Li_{0.968}Al_{0.294}Ni_{0.191}Mn_{1.484}O_{3.932}$	8.172	0.978	0.046
$LiAl_{0.4}Ni_{0.1}Mn_{1.5}O_4$	$Li_{0.974}Al_{0.391}Ni_{0.086}Mn_{1.483}O_{3.921}$	8.187	0.930	0.054
$LiCu_{0.1}Ni_{0.4}Mn_{1.5}O_4$	$Li_{0.987}Cu_{0.094}Ni_{0.393}Mn_{1.493}O_{3.961}$	8.173	0.901	0.044
$LiCu_{0.2}Ni_{0.3}Mn_{1.5}O_4$	$Li_{0.976}Cu_{0.183}Ni_{0.289}Mn_{1.496}O_{3.939}$	8.189	0.828	0.055
$LiCu_{0.3}Ni_{0.2}Mn_{1.5}O_4$	$Li_{0.978}Cu_{0.279}Ni_{0.188}Mn_{1.491}O_{3.923}$	8.195	0.741	0.089
$LiCu_{0.4}Ni_{0.1}Mn_{1.5}O_4$	$Li_{0.966}Cu_{0.387}Ni_{0.092}Mn_{1.503}O_{3.957}$	8.203	0.791	0.133

Chemical compositions as determined by ICP-MS.

material with 10 wt.% conductive carbon black and 5 wt.% PVdF binder in NMP on an aluminum foil, drying overnight at 120 °C in an oven, roller-pressing the dried coated foil, and punching out circular discs. Cell assembly was done in an argon-filled glove box (VAC, MO 40-1) that contained <2 ppm oxygen and moisture. The cells were cycled at a 0.1 C rate between 3.30 and 4.95 V in a multi-channel battery tester (Maccor 4000). The slow scan cyclic voltammetric (SSCV) experiments were performed in a three-electrode glass cell placed inside the glove box. The cathodes were prepared as described above, but coated on both sides of the aluminum foil. The cells for SSCV studies were assembled inside the glove box with lithium metal foil serving as both counter and reference electrodes. The electrolyte used was the same as that for the coin cell. Cyclic voltammograms were run on a Solartron 1287 electrochemical interface at a scan rate of 0.1 mV/s between 3.00 and 5.10 V. The impedance spectra were recorded with 2032-type coin cells on a Solartron 1250/1287 set-up between 65 kHz and 0.001 Hz. The cells were galvanostatically charged and discharged to various depths of intercalation and deintercalation prior to recording the impedance plots.

3. Results and discussion

3.1. X-ray diffraction

Typical powder X-ray diffraction patterns recorded for the Fe-substituted $LiMn_2O_4$ compositions are shown in Fig. 1.
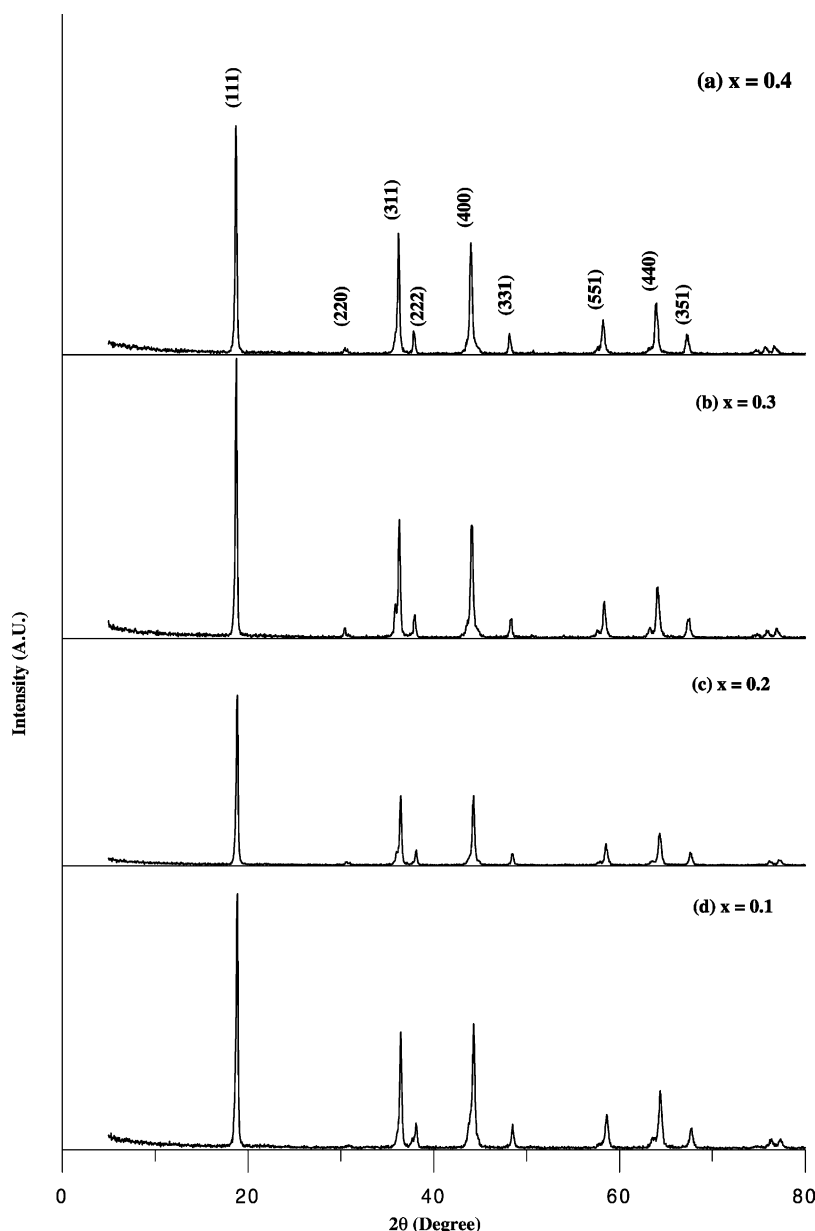
Fig. 1. Powder X-ray diffractograms of $LiFe_yNi_{0.5-y}Mn_{1.5}O_4$ ($y = 0.0$–0.4).

The diffraction patterns of the other substituted systems were similar, with all the peaks indexable in the Fd3m space group with a cubic lattice. The Al-substituted compositions, especially at the higher Al concentrations, gave a few minor additional peaks, suggesting the presence of some extraneous phases in the material. Similarly, the Fe-substituted compounds also had additional diffraction peaks corresponding to small amounts of Li_2MnO_3 coexisting with the spinel phases. Similar observations have been recorded with Cu-substituted $LiMn_2O_4$ synthesized by a solid-state method [16,19].

The lattice parameter a calculated by a least square method showed a linear increase with an increase in the substituent ion (M) concentration in $LiM_yNi_{0.5-y}Mn_{1.5}O_4$. This is a characteristic feature of solid solutions that obey Vegard's law, according to which some material parameters, such as lattice constants, vary linearly with the mole fraction of the substituent species. However, in the case of the Al-substituted systems, a deviation from Vegard's law was observed (Table 1). The deviation from Vegard's law in this case may have been related to the presence of extraneous phases, especially in those compositions with higher concentrations of Al. According to Myung et al. [20], these additional diffraction lines can be ascribed to γ-$LiAlO_2$. It is generally known that the replacement of the transition metal site with Al is not easy because impure phases such as Al_2O_3 and γ-$LiAlO_2$ can easily form at high temperatures such as those employed here [20].

The site occupancy of the substituent ions in the host matrix is an important factor, which determines the electrochemical properties of the system. Ohzuku et al. [13] used the integrated intensity ratios of close-lying peaks in the XRD spectra to determine the extent of occupancy of substituent ions. In the case of the ideal $LiMn_2O_4$ structure, the lithium and manganese ions are located in the 8a tetrahedral and 16d octahedral sites, respectively, in a cubic close packed array of O^{2-} ions, which occupy the 32e sites [28,29]. The objective of the present study is to partially replace the Mn ions in the 16d sites of the $LiMn_2O_4$ matrix with the substituent ions. Occupancy of the substituent ions in the 8a lithium sites will lead to unfavorable electrochemical results.

According to Ohzuku et al. [13], the integrated intensity ratios of the (4 0 0)/(3 1 1) and (2 2 0)/(3 1 1) peaks are indices of the extent of occupancy of the substituent ions in the 8a lithium sites. In the case of the $LiFe_yNi_{0.5-y}Mn_{1.5}O_4$ samples, the integrated intensity ratio (4 0 0)/(3 1 1) dropped when the Fe content was increased. However, the (2 2 0)/(3 1 1) generally increased with an increase in the Fe content. It can be seen from the XRD patterns that the intensity of the (2 2 0) peak increased with the Fe content. Such an increase in the intensity of the (2 2 0) peak and the corresponding increase in the (2 2 0)/(3 1 1) intensity ratio should indicate increased occupancy of the substituent Fe in the 8a lithium lattice sites as the Fe content is increased. This was complemented by a decrease in the (4 0 0)/(3 1 1) intensity ratios.

The intensity ratios for the various products are summarized in Table 1. It can be seen from the table that the trend was generally the same in the case of the spinels co-substituted with Cu, Al, and Mg also. Thus, it appears that all the co-substituents show a propensity for 8a site occupation as their concentrations are increased.

3.2. Cyclic voltammetry

The cyclic voltammograms were recorded between 3.00 and 5.10 V. Although electrolyte decomposition was a possibility at such high voltages, there was no evidence of such a process in the voltammograms. In fact, $LiPF_6$-based electrolytes, such as the one used in this study, are fairly tolerant to high voltages [30]. The cyclic voltammograms recorded for the various substituted systems are shown in Fig. 2. As can be seen from the figure, there are mainly two regions of electrochemical activity: one, around 4.0 V, corresponding to the Mn^{4+}/Mn^{3+} couple, and the other, above 4.4 V (hereinafter referred to as the 5-V region), corresponding to the oxidation/reduction of the substituent ions. In the present study, apart from the common nickel ion substituent, the other substituent ion was either a transition metal ion or a non-transition metal ion. Hence, the electrochemical characteristics of the materials must reflect, in addition to the redox reactions of Mn and Ni, those of the additional substituent species. Such observations have been made with $LiMn_2O_4$ substituted with Ni/Cr/Cu/Fe/Zn [11].

Fig. 2a and b show the cyclic voltammograms of $LiNi_{0.4}Fe_{0.1}Mn_{1.5}O_4$ and $LiNi_{0.1}Fe_{0.4}Mn_{1.5}O_4$, respectively. They show a typical 4-V peak corresponding to the Mn^{4+}/Mn^{3+} couple, and a 5-V peak corresponding to the redox reactions of the Ni and Fe ions. According to Ohzuku et al. [13], the Ni-substituted $LiMn_2O_4$ system presents a single oxidation–reduction reaction above 4.5 V, but the presence of two redox regions around 5 V in the cyclic voltammogram of $LiNi_{0.4}Fe_{0.1}Mn_{1.5}O_4$ indicates that the co-substituent Fe altered the electrochemical properties of the system. A shoulder that appears ca. 5.0 V is attributable to the oxidation of Fe^{3+} to Fe^{4+} [13]. The prominent double peak observed in the Ni-rich composition is similar to that observed by others who studied Ni-doped lithium manganese oxide spinels [3,26]. According to Striebel et al. [26], the double peak may be due to the progressive oxidation of Ni^{2+} to Ni^{4+} through Ni^{3+}. An increase in the Fe content from 0.1 to 0.4 resulted in a single high-potential peak (5.07 V). Simultaneously, the increased Fe stoichiometry from 0.1 to 0.4 resulted in an order of magnitude increase in the value of the currents for the 4-V redox peaks. The increased currents in the 4-V region as the Fe content was increased corresponded to increased amounts of Mn^{3+} in the compounds. However, the 4-V peak oxidation peak shifted to higher potentials, suggesting that a higher potential is required to extract lithium from the matrix of the Fe-substituted compounds. Simultaneously, the corresponding reduction peak shifted to a lower potential range. Thus, the reversibility
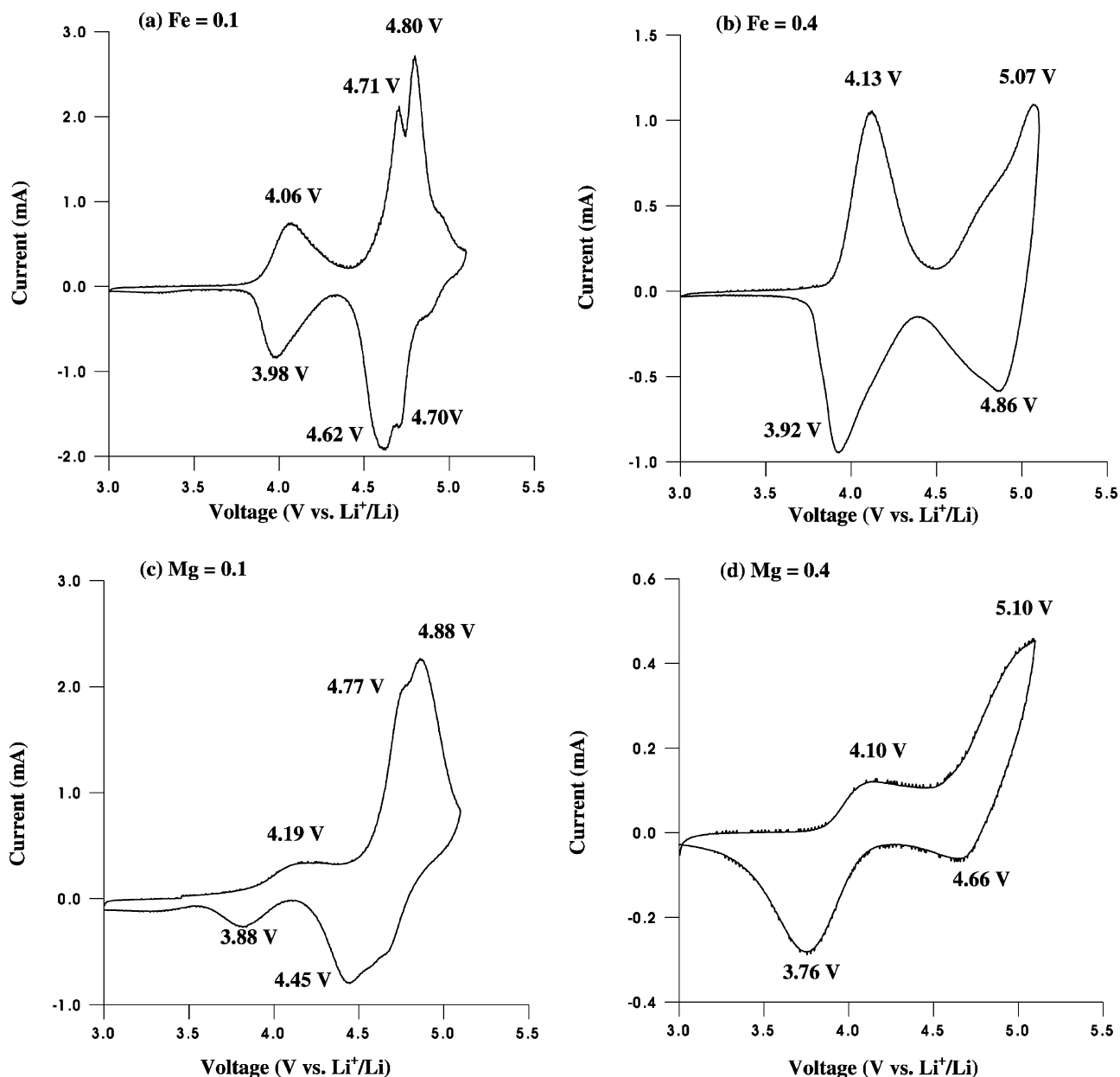
Fig. 2. Cyclic voltammograms of $LiM_yNi_{0.5-y}Mn_{1.5}O_4$. M = Fe, Mg, Al, or Cu; $x = 0.1–0.4$.

of the 4-V couple suffers upon increasing the amount of Fe in the spinel. Clearly, Fe as a dopant influences the electrochemical characteristics of the Mn^{4+}/Mn^{3+} couple. A similar effect was noticed in our studies on $LiFe_yCr_{0.5-y}Mn_{1.5}O_4$ [31].

The effect of substituting Ni with Mg is shown in Fig. 2c and d. The 4-V peak appears very suppressed compared to the higher-voltage peaks in accordance with the fact that the divalent ion substituents, Ni and Mg, lead to a decline in the number of electrochemically active Mn^{3+} ions, which get oxidized to 4-V-inactive Mn^{4+} ions. The appearance of a shoulder at 4.77 V in the cyclic voltammogram of $LiNi_{0.4}Mg_{0.1}Mn_{1.5}O_4$ probably represents the first step in the progressive oxidation of Ni^{2+} to Ni^{3+} and then to Ni^{4+}

[21]. Similar to when Fe was substituted, the higher-voltage peak (at 4.88 V) gets shifted to higher potentials (5.10 V) as the Mg content is increased. This is in accordance with the general observation that non-transition metal ions shift the operating voltage to higher values.

In the case of the Al-substituted compounds (Fig. 2e and f), cyclic voltammetry showed an increase in the 4-V peak current as the Al content was increased. This was expected since the increased replacement of the divalent Ni by the trivalent Al should result in increased amounts of the 4-V-active Mn^{3+} ions. For example, if all the substituent ions were to occupy only the 16d octahedral sites, the compound with $y = 0.1$ should be represented as $[Li]_{8a}$-$[Al_{0.1}^{3+} Ni_{0.4}^{2+} Mn_{0.1}^{3+} Mn_{1.4}^{4+}]_{16d}[O_4]_{32e}$, and that with $y = 0.4$ as
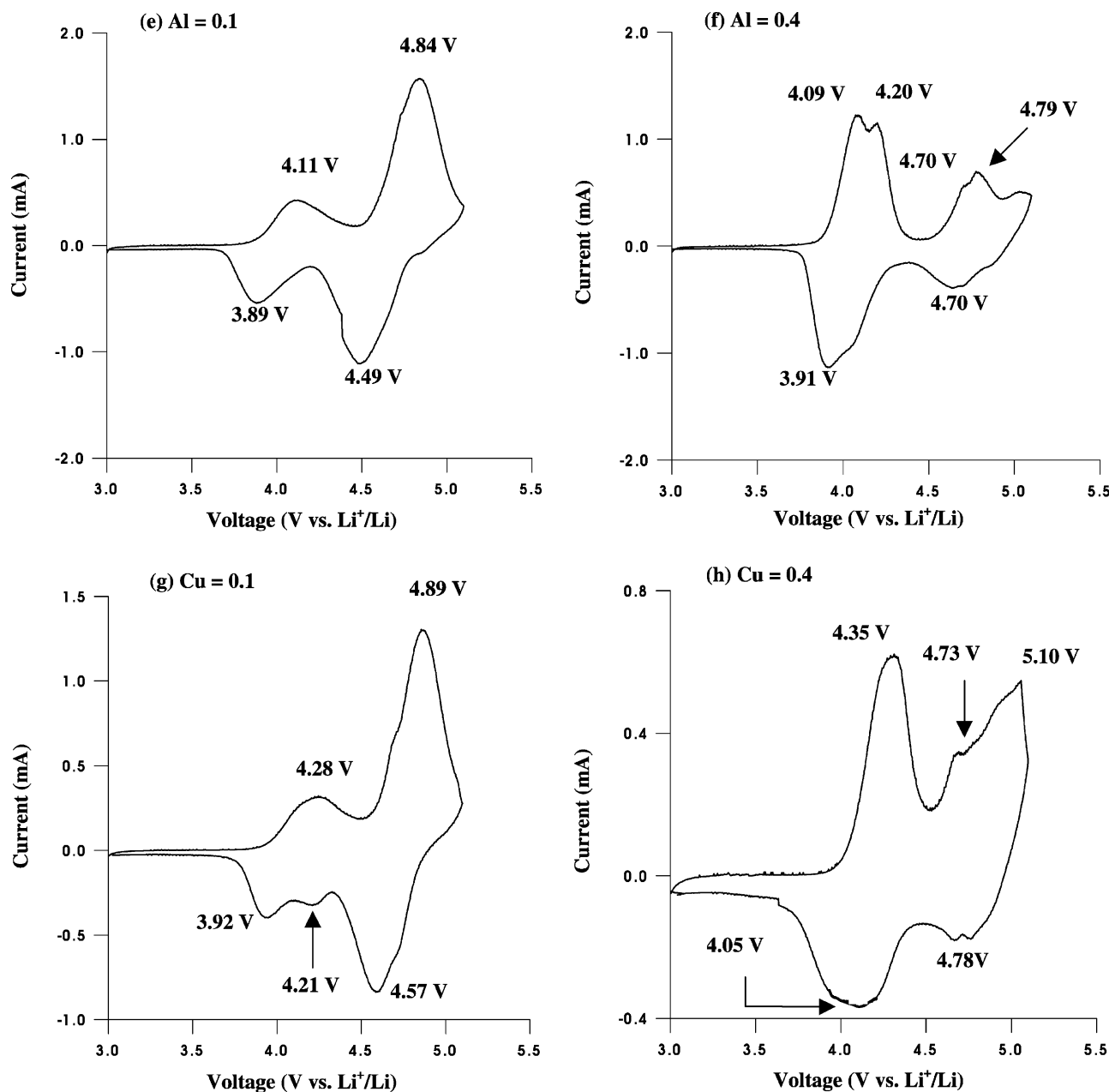
Fig. 2. (*Continued*).

$[Li]_{8a}[Al^{3+}_{0.4} Ni^{2+}_{0.1} Mn^{3+}_{0.4} Mn^{4+}_{1.1}]_{16d}[O_4]_{32e}$. Al substitution led to a diminution in the peak area corresponding to the 5-V redox couple, whose potential was shifted to 4.84 V. It can also be seen that an increase in the Al content to $y = 0.4$ led to a splitting of the 4-V peak, a characteristic of the $LiMn_2O_4$ system [26]. According to Sigala et al. [30], the 5-V activity is related to the Ni^{4+}/Ni^{2+} redox system. The two-electron redox couple in this region is assumed based on XPS data, which show only the presence of Ni^{2+} in $LiNi_{0.5}Mn_{1.5}O_4$ [32]. However, in addition to the split peaks corresponding to the $Ni^{2+}–Ni^{3+}–Ni^{4+}$ reactions, a peak appears ca. 5.1 V. The low reduction currents corresponding to this peak show the limited reversibility of this process. This is in accordance

with the results of Shao-Horn and Middaugh [33], who investigated the $Li/LiAl_{0.5}Mn_{1.5}O_4$ system. In fact, the 5-V peak, observed with $LiAl_{0.5}Mn_{1.5}O_4$ as well as in our studies, is totally unexpected given that there is no conventional-type redox couple corresponding to this potential region in these systems. According to Shao-Horn and Middaugh [33], the electrochemical reactions in the 5-V region in substituted $LiMn_2O_4$ spinels may have more to do with redox reactions of the oxygen lattice brought about by substitutions in the spinel framework than with the conventional redox reactions of the transition metal species. The authors hypothesize that an increase in the Mn^{4+} concentration in the spinel due to substitution or extensive lithium

deintercalation is a prerequisite for the occurrence of electrochemical processes around 5 V [33]. Ceder and coworkers' [34] ab initio calculations show that the 5-V activity is strongly influenced by the oxygen lattice. However, it seems unlikely that any reversibility in the 5-V region can be attained without a transition metal ion compensating for the charge imbalance created during the lithium intercalation/deintercalation processes.

Fig. 2g and h depict the effect of Cu on the electrochemical behavior of $LiNi_{0.5-y}Cu_yMn_{1.5}O_4$ spinels. In all the compositions, the 4-V activity appears suppressed because of the oxidation of the electrochemically active Mn^{3+} to Mn^{4+} in order to compensate for the charge imbalance arising from the replacement of a trivalent Mn ion by the divalent Cu and Ni ions. Interestingly, incorporating Cu shifted the 4-V peak to a potential as high as 4.35 V, which means that the 4-V activity of the spinel, attributed to the Mn^{4+}/Mn^{3+} redox couple, was not altogether lost and suggests that not all the Mn was in the 4+ state. Our deduction is in agreement with the results of Ein-Eli et al. [18], although it contradicts the findings on similar materials reported by other groups [23,24,35]. A similar shift in the 4-V peak was noticed by Ein-Eli and Howard [16] in their studies with Cu-substituted $LiMn_2O_4$. The shift in the 4-V peak of the Mn^{4+}/Mn^{3+} couple with increased substitution has been observed by a number of groups [26,35,36]. The single peak at 4.89 V obtained with $LiNi_{0.4}Cu_{0.1}Mn_{1.5}O_4$ seems to be a combination of the oxidation peaks for the Ni substituent, at 4.7 V [23,24,32,35], and the Cu substituent, at 4.9 V [11,16–18]. The high-potential single peak shifted to 5.10 V with a shoulder at 4.73 V when the composition was changed to $LiNi_{0.1}Cu_{0.4}Mn_{1.5}O_4$. It must be noted that the octahedral site energies for Cu^{2+} and Al^{3+} are high. Hence, the decrease in the capacity derived from the compositions containing these substituents is more likely due to the high potentials required to extract lithium from such materials.

From the foregoing, it is clear that the 4-V capacity in these materials arises from the Mn^{4+}/Mn^{3+} couple and that the 5-V capacity arises from the substituent ions. In the case of the materials simultaneously substituted with Ni and a transition metal, the 5-V capacity results from a cumulative contribution from both the substituent ions. However, in the case where the co-substituent is a non-transition metal, contributions other than those from the oxidation–reduction of the substituents come into play. The co-substituent alters the electrochemical behavior of both Mn^{4+}/Mn^{3+} and Ni^{4+}/Ni^{2+} couples. Irrespective of whether it is a transition or a non-transition metal, the effect is more pronounced in the 5-V region. Although tapping the full capacities from these substituted materials requires a stable electrolyte, they do represent a class of materials for high energy density lithium batteries.

3.3. Charge–discharge studies

Electrochemical charge–discharge studies were performed in a galvanostatic mode between 3.30 and 4.95 V

at a 0.1 C rate. The upper voltage was limited to 4.95 V for fear of possible electrolyte decomposition, especially upon extended cycling. Typical first-cycle discharge profiles for all the substituted systems are shown in Fig. 3. Reflecting the cyclic voltammograms, the charge–discharge curves also showed two voltage plateaus in the 4- and 5-V regions. For capacity calculations, the 4-V region is defined as the region between 3.00 and 4.40 V, and the 5-V region as that between 4.40 and 4.95 V. The theoretical capacities in the two regions were calculated under the premise that the substituent ions replaced the Mn^{3+} in the octahedral sites. The targeted formulae were used for the calculation of the theoretical capacities, because not knowing the amount of the Mn^{3+} and Mn^{4+} species in the compounds precludes such a calculation, especially in the 4-V region, based on the chemical compositions actually obtained.

For comparison, the cycling performance of an unsubstituted $LiMn_2O_4$ sample was also studied. The charging and discharging in this case was carried out between 3.0 and 4.2 V at a 0.1 C rate. The first discharge capacity of the unsubstituted material was 108 mAh/g, while the corresponding value in the 4-V region for a $LiNi_{0.5}Mn_{1.5}O_4$ sample was 27.2 mAh/g. As may be expected, introducing the divalent Ni in the spinel lattice at a concentration of 0.5 atom/molecule eliminates all the Mn^{3+} ions, rendering the compound 4-V-inactive. However, the fact that a small capacity still appears in the 4-V region suggests that not all the Mn in the spinel is present in the 4+ state. As noted above, our results are in agreement with those of Ein-Eli et al. [18], although they are different from those of other groups [23,24,35]. While substituting another divalent ion for Ni should in no way change the 4-V activity of $LiNi_{0.5}Mn_{1.5}O_4$, any substitution with a trivalent ion should result in the reduction of an equivalent amount of Mn^{4+} to Mn^{3+}, yielding materials with 4-V activity. From Table 2, it can be seen that an increase in the co-substituent content in $LiM_yNi_{0.5-y}Mn_{1.5}O_4$ (M = Mg or Cu) does not result in any appreciable enhancement in the 4-V capacity, although the capacity enhancement is slightly more in the case of the Cu-substituted samples. Cu-substituted $LiMn_2O_4$ systems are known to deliver 4-V capacities higher than their theoretically possible limits [17,19]. The results are inconsistent with the simple spinel structure that was assigned to the Cu-substituted Li–Mn–O spinels. According to Ein-Eli and coworkers [16–18], the cation distribution in the Cu-substituted spinels is extremely complex, attributable to the incomplete incorporation of Cu into the spinel because of the stability and the relatively low reactivity of the CuO precursor. On the other hand, when the co-substituent content in $LiM_yNi_{0.5-y}Mn_{1.5}O_4$ (M = Al or Fe) is increased, there is a corresponding increase in the 4-V capacity. The 4-V capacity is commensurate with an increase in the amount of Mn^{3+} as the divalent nickel ions are replaced.

The capacity trend in the 5-V region also mirrors the cyclic voltammetric data. The parent compound, $LiMn_2O_4$, had no 5-V activity. However, $LiNi_{0.5}Mn_{1.5}O_4$ should, in
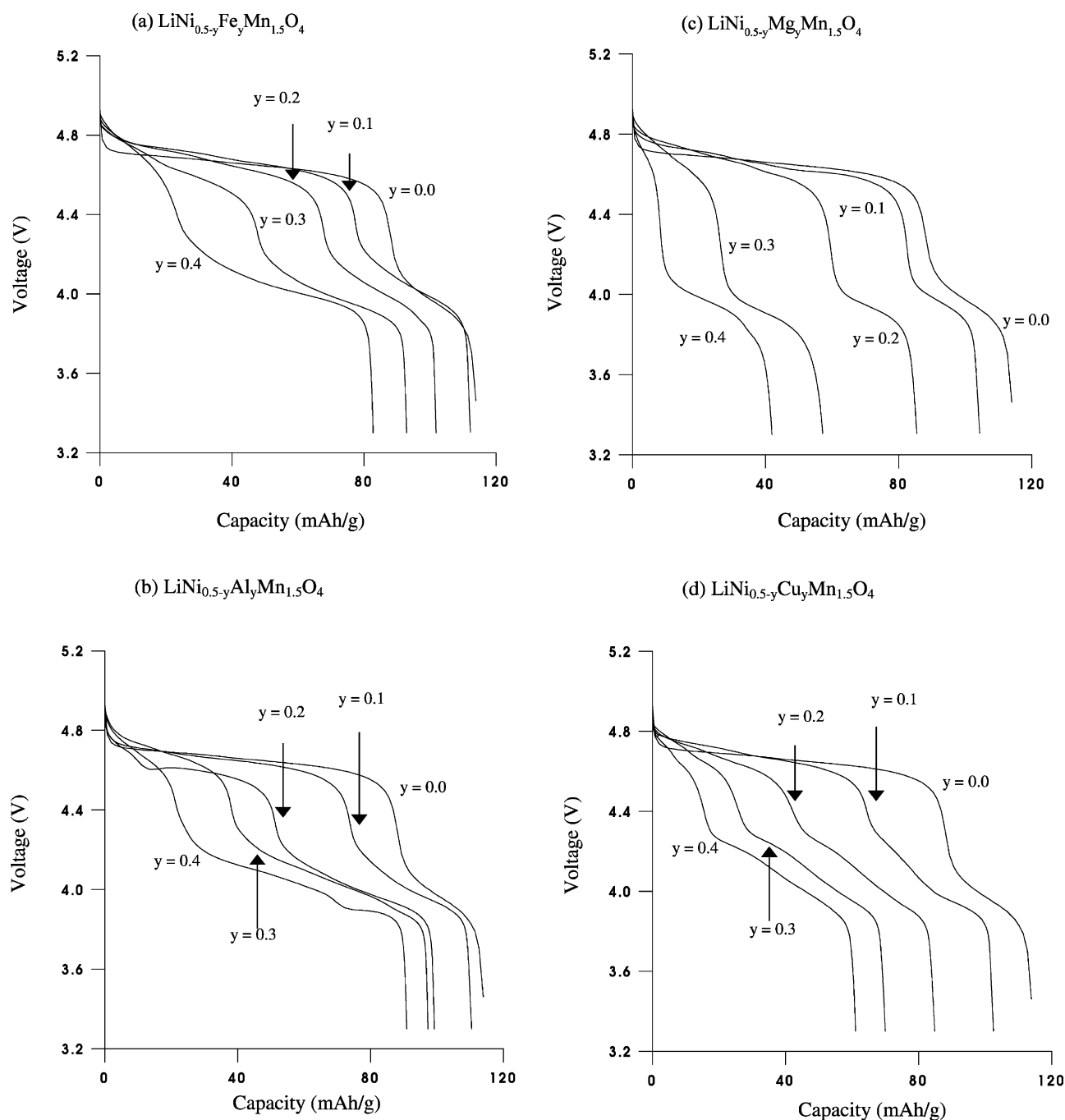
Fig. 3. A conspectus of the first-cycle discharge curves of the various doped systems. Dopant: (a) Fe; (b) Al; (c) Mg; and (d) Cu. Cycling conditions: 3.30–4.95 V @ 0.1 C rate.

theory, exhibit its entire capacity in the 5-V region because it is bereft of the 4-V-active Mn^{3+} ion and has the Ni^{4+}/Ni^{2+} couple active in the 5-V region. Moreover, if the 5-V capacity-yielding reaction is supposed to involve the oxidation of Ni^{2+} to Ni^{4+}, the capacity should be double that which may be expected from a single-electron transfer reaction such as the one involving the Fe substitutent. However, much lower capacities than the theoretically expected ones could only be realized for $LiNi_{0.5}Mn_{1.5}O_4$ in the 5-V region. It can be seen from Table 2 that for all the

materials, the 5-V capacity decreases as the co-substituent content is increased, because as the co-substituent content (y) is increased, there is a corresponding decrease in the Ni content ($0.5 - y$), which contributes to the 5-V capacity. The decrease in the 5-V capacity is all the more conspicuous because the displaced ion is a high-capacity vehicle by virtue of its two-electron transfer reaction. Thus, even when the co-substituent is a 5-V-active species like Fe or Cu, capacity is reduced more because the co-substituents can deliver capacity only through a one-electron transfer reaction.

Table 2
The theoretical and observed first-cycle capacities of the various $LiM_xNi_{0.5-x}Mn_{1.5}O_4$ compositions

Composition	4-V capacity (mAh/g)		5-V capacity (mAh/g)		Observed cumulative capacity (mAh/g)
	Theoretical	Observed	Theoretical	Observed	
$LiMn_2O_4$	148.2	108.0	–	–	108.0
$LiNi_{0.5}Mn_{1.5}O_4$	0.0	27.2	146.7	86.8	114.0
$LiFe_{0.1}Ni_{0.4}Mn_{1.5}O_4$	14.7	36.4	132.4	80.7	117.1
$LiFe_{0.2}Ni_{0.3}Mn_{1.5}O_4$	29.4	37.6	117.7	65.4	103.0
$LiFe_{0.3}Ni_{0.2}Mn_{1.5}O_4$	44.2	47.3	103.3	45.7	93.0
$LiFe_{0.4}Ni_{0.1}Mn_{1.5}O_4$	59.0	59.7	88.6	23.3	83.0
$LiAl_{0.1}Ni_{0.4}Mn_{1.5}O_4$	14.9	37.1	119.4	72.9	110.0
$LiAl_{0.2}Ni_{0.3}Mn_{1.5}O_4$	30.4	48.8	91.2	50.2	99.0
$LiAl_{0.3}Ni_{0.2}Mn_{1.5}O_4$	46.4	58.9	61.9	38.1	97.0
$LiAl_{0.4}Ni_{0.1}Mn_{1.5}O_4$	63.1	69.3	31.5	21.7	91.0
$LiMg_{0.1}Ni_{0.4}Mn_{1.5}O_4$	0.0	23.3	119.6	80.7	104.0
$LiMg_{0.2}Ni_{0.13}n_{1.5}O_4$	0.0	27.4	91.5	57.6	85.0
$LiMg_{0.3}Ni_{0.2}Mn_{1.5}O_4$	0.0	32.1	62.2	24.9	57.0
$LiMg_{0.4}Ni_{0.1}Mn_{1.5}O_4$	0.0	34.0	31.7	8.0	42.0
$LiCu_{0.1}Ni_{0.4}n_{1.5}O_4$	0.0	38.7	131.6	64.3	103.0
$LiCu_{0.2}Ni_{0.3}Mn_{1.5}O_4$	0.0	42.9	116.8	42.1	85.0
$LiCu_{0.3}Ni_{0.2}Mn_{1.5}O_4$	0.0	44.1	101.9	25.9	70.0
$LiCu_{0.4}Ni_{0.1}Mn_{1.5}O_4$	0.0	45.5	87.1	15.5	61.0

It can also be seen from Table 2 that the cumulative capacity of the spinel increases when the extent of substitution with Ni is increased from 0.0 to 0.5 atom/molecule. At the latter composition, theoretically, there is only one active species: the 5-V-oxidizable Ni^{2+} species, whose two-electron transfer oxidation to Ni^{4+} should result in higher capacities. In fact, the first-cycle discharge capacity of $LiNi_{0.5}Mn_{1.5}O_4$ was 114 mAh/g versus 108 mAh/g for $LiMn_2O_4$. It must be noted that even higher capacities were obtained with $LiFe_{0.1}Ni_{0.4}Mn_{1.5}O_4$ (117 mAh/g) and $LiAl_{0.1}Ni_{0.4}Mn_{1.5}O_4$ (110 mAh/g). Thus, the trivalent substituents seemed to aid in an increased utilization of the 5-V capacity. Higher capacities at higher voltages should translate into higher power densities for the Ni-substituted spinels.

The results of extended cycling studies show that the unsubstituted spinel gave a cumulative first-cycle discharge capacity of 108 mAh/g, which faded to 90 mAh/g in the 25th cycle, registering a charge retention of 84%. The corresponding values for $LiNi_{0.5}Mn_{1.5}O_4$ were 114 and 110 mAh/ g and 97%. Thus, substitution with Ni enhanced the first cycle capacity as well as the cyclability of the spinel. Gao et al. [24] and Zheng et al. [35] have shown that $LiNi_{0.5}Mn_{1.5}O_4$ can deliver as much as 120 mAh/g at high potentials (4.6–4.7 V) and that its stability is limited. In the case of the Fe- and Al-substituted compositions with $y = 0.1$, there was an initial surge in the capacities (117 and 110 mAh/g, respectively). However, as the y values were increased, the capacities of the Fe- and Al-substituted materials dropped. In the case of the Fe-doped compositions, the fall in capacity with an increase in the y value is a consequence of the increased propensity of these ions to occupy the 8*a* lithium sites as their concentrations are increased. Their occupancy in the lithium sites can impede transport of the Li ions during the charge–discharge processes. The higher potentials required to remove lithium ions from the Fe-substituted compounds, as seen from our cyclic voltammetric studies, must also be considered. The values of the percentage capacity retention in the 60th cycle for the Fe-substituted system increased from 78 to 81 as the y value was increased from 0.1 to 0.4. Fe as a substituent in the spinel is believed to form a slightly distorted spinel structure [14], thereby conferring increased stability to the spinel. Song et al. [15] have demonstrated that Fe substitution renders the spinel more cyclable. However, the improvement in capacity retention must be viewed against the backdrop of a considerable reduction in the first-cycle capacity as the y values were increased. The first-cycle capacity fell from 117 to 83 mAh/g when the Fe content was increased from 0.1 to 0.4. Nevertheless, substitution with Fe does bestow an increase in the cycling stability to the cathode material.

It can be seen from Table 2 that the calculated capacity of $LiAl_{0.2}Ni_{0.3}Mn_{1.5}O_4$ is 121.6 mAh/g and that for $LiAl_{0.4}Ni_{0.1}Mn_{1.5}O_4$ is 94.6 mAh/g. The respective observed capacities are 99 and 91 mAh/g. Therefore, although the capacity fell with an increase in the Al content, the observed capacity is closer to the theoretical capacity when $y = 0.4$ than in the case when $y = 0.1$. However, our X-ray diffraction results show that at the higher concentration, Al exhibited a propensity for occupying the 8*a* sites. Thus, it can be inferred that the presence of Al in the 8*a* sites does not hinder the transport of lithium. In the case of the Al-substituted system, the capacity retention decreased from 78 to 71% over 60 cycles when the Al content, y, was increased from 0.1 to 0.4. As can be seen from Table 1, the values of the lattice parameter, a, for all the Al-substituted compositions are
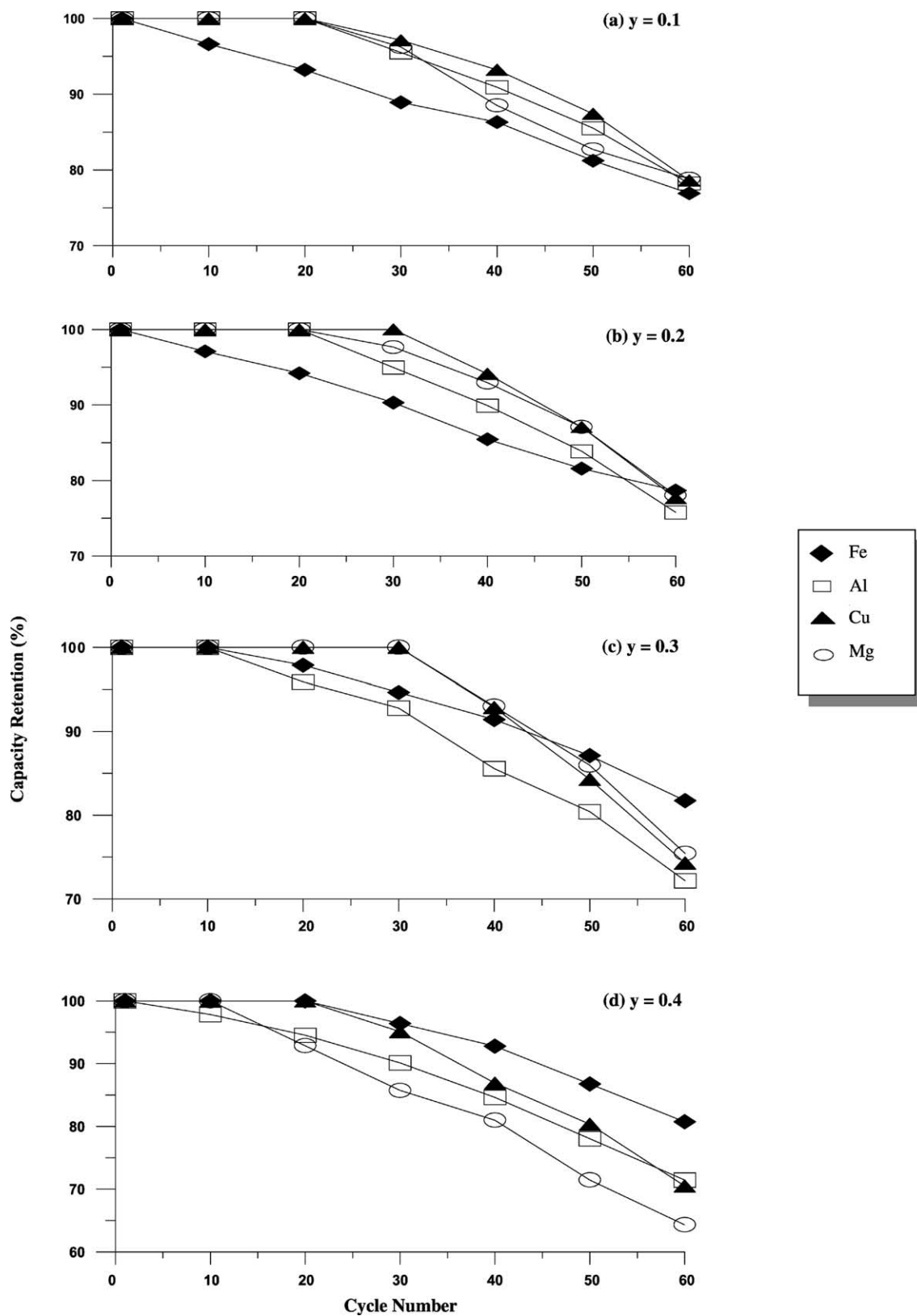
Fig. 4. Plots of capacity retention vs. cycle number for the various compositions. Cycling conditions: 3.30–4.95 V @ 0.1 C rate.
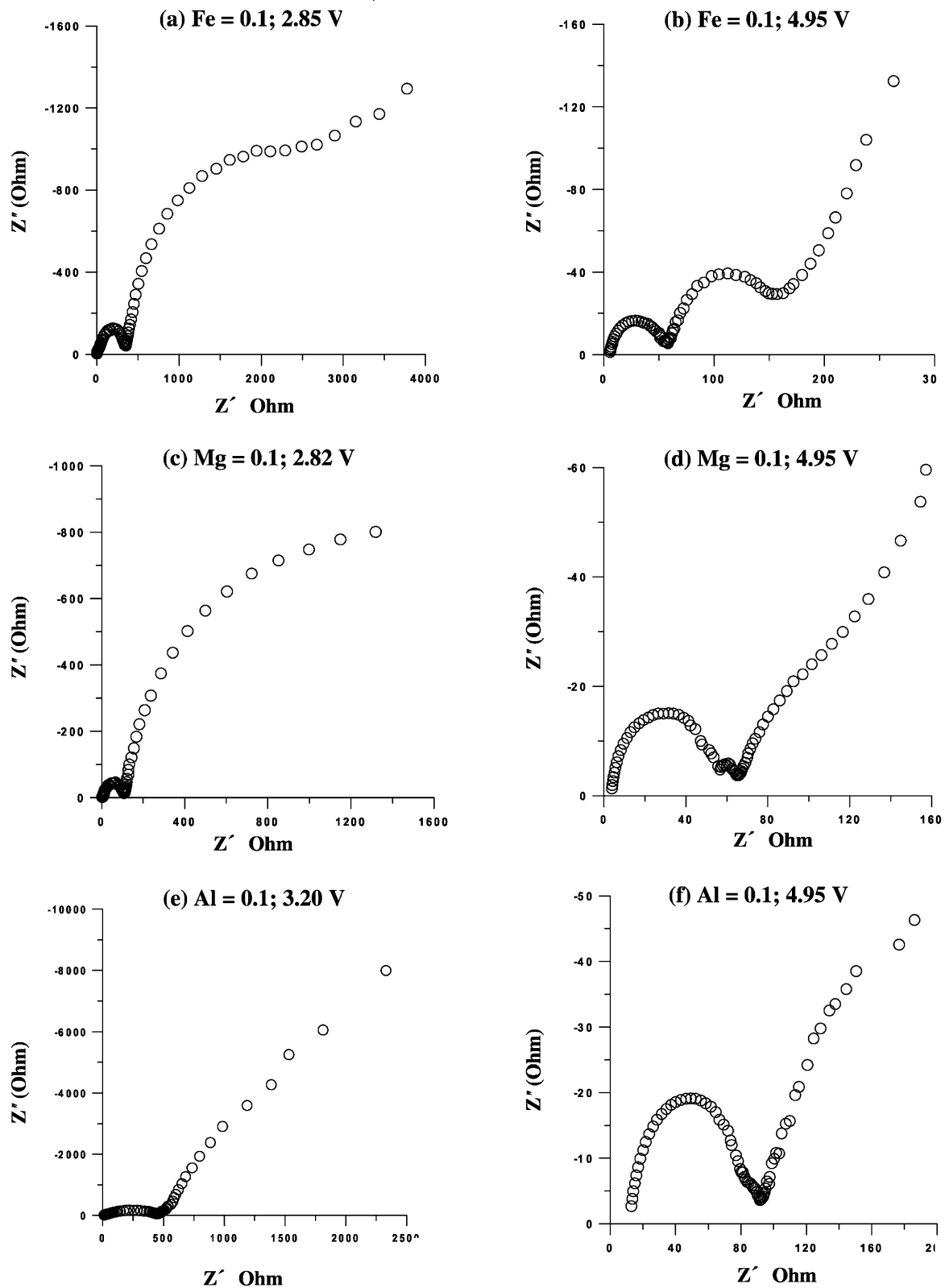
Fig. 5. Nyquist plots of $LiM_yNi_{0.5-y}Mn_{1.5}O_4$ (M = Fe, Mg, Al, and Cu) systems recorded at different voltages.
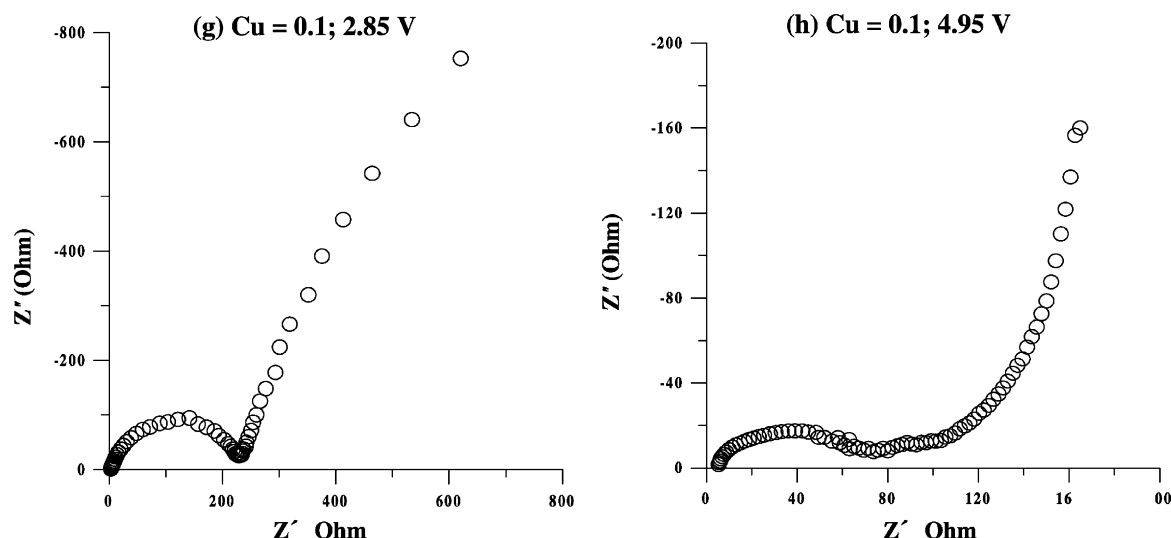
Fig. 5. (*Continued*).

lower than those for the undoped $LiMn_2O_4$. However, they are larger than that for $LiNi_{0.5}Mn_{1.5}O_4$. This suggests that the Al-substituted compositions may provide a stabler structure than $LiMn_2O_4$ for reversible lithium intercalation, but a less favorable structure than $LiNi_{0.5}Mn_{1.5}O_4$. Perhaps, only the $LiNi_{0.5}Mn_{1.5}O_4$ composition is expected to enhance the capacity and stability of the spinel at high voltages. The enhanced structural stability of Al-doped $LiMn_2O_4$ has been demonstrated in the 4-V region (e.g. [12,37]). However, Lee and Yoshio [38], who demonstrated the excellent cyclability of $LiAl_{0.1}Mn_{1.9}O_2$ in the 4-V region, also observed a drop in the cyclability of Li–Mn–O spinels in the 3-V region. In our case, a simultaneous doping of $LiMn_2O_4$ with Ni and Al is found to reduce the cyclability in the 5-V region. Thus, the stabilizing effect of the Al dopant seems to depend on the potential range studied. It was observed that the capacities of the Al-, Mg-, and Cu-substituted materials registered a general increase from the first cycle to the 10th, followed by a slow decay in subsequent cycles.

As in the case of the Al-substituted system, the materials substituted with Mg or Cu also displayed reduced capacity retention, dropping from 79% ($y = 0.1$) to 71% ($y = 0.4$) for the Mg-substituted materials, and 79% ($y = 0.1$) to 70% ($y = 0.4$) for the Cu-substituted materials over 60 cycles. Again, the palpably poor first cycle capacities obtained at high y values need to be noted, their values dropping by as much as 60 and 41% for the Mg- and Cu-substituted systems, respectively, as the y value was increased from 0.1 to 0.4. The lowering of the capacity with an increase in the Cu content is in agreement with the findings of Ein-Eli et al. [18]. The lower capacity for the copper-rich spinels is related to the reduced capacities obtainable from the one-electron redox process associated with the Cu^{3+}/Cu^{2+} couple [39] compared to the two-electron redox process associated with the Ni substituent [24]. Fig. 4 illustrates the cycling behavior of the four substituted systems.

3.4. Electrochemical impedance spectroscopy

EIS measurements were made both in the as-assembled and fully charged states (charged to 4.95 V) with the intent of understanding the various electrochemical processes taking place. The Nyquist plots recorded for the various doped systems are shown in Fig. 5. The following observations can be made from the plots. All the Nyquist plots showed one or two semicircles and a Warburg impedance associated with the diffusion of lithium ions in the oxide matrix. The first semicircle is associated with the passivation layer on the electrode. The second one is associated with the charge-transfer resistance coupled with a capacitance at the surface film/cathode particle interface arising from surface-adsorbed species. The electrolyte resistance, R_e, does not seem to depend on the voltage at which the impedance spectra is recorded. This is expected because the electrolyte concentration remains invariant, and variations in the lithium content of the electrodes need not influence the electrolyte conductivity. The second semicircle in the Nyquist plots recorded at 4.95 V showed some variations depending on whether the co-substituent was a transition or a non-transition metal ion. This semicircle is associated with the 5-V activity of the materials under study. It is a well-defined one for the Fe-substituted system, while for the Cu-substituted system it is depressed. In the case of Mg and Al-substituted systems, the second semicircle is hardly discernible. For all the systems, the charge transfer resistance diminished in the charged state, which indicates that the materials became more conductive at the higher state-of-charge.

In their highly deintercalated states, the materials turned into good conductors, a fact that can impact on the high-drain capability of the system. The capacitance associated with the first semicircle is usually in the order of microfarads and is related to the surface film on the oxide. On the other hand, the charge transfer process in a 3*d* transition metal ion

oxide is around several mF as evidenced from the second semicircle [40]. Since the surface film is expected to grow as the charging voltage is raised, the resistance represented by the first semicircle must be higher for the fully charged cathode as compared to the pristine cathode. However, Fig. 5 shows that the pristine samples exhibited higher resistances. This apparent contradiction may be explained as follows. Based on their FTIR studies, Aurbach et al. [41] showed that pristine $LiCoO_2$ and $LiMn_2O_4$ were covered with a layer of Li_2CO_3, most probably formed by the interaction of the basic $LiMO_x$ oxide with the acidic CO_2 in the atmosphere. This layer is a compact layer offering a high resistance. Upon charging, the electrodes become covered with a surface layer of RCOOLi due to interaction of the cathode material with the EC-DMC electrolyte [42]. At high charging voltages, the deintercalation processes is accompanied by changes in volume of the cathode and thickness of its surface layer [42]. These changes together with the numerous by-pass channels formed for lithium migration could account for the reduced resistance of the film at the cathode surface at high charging voltages [42].

4. Conclusions

$LiNi_{0.5-y}M_yMn_{1.5}O_4$ spinels, where M = Fe, Mg, Al, or Cu, and y = 0.0–0.4, have been synthesized via a conventional ceramic route and studied as high-voltage cathode materials. Powder X-ray diffraction studies showed that phase-pure products were obtained when the substituents were Mg and Cu. However, all the substituents displayed a propensity for the 8*a* tetrahedral site, especially at higher concentrations. Cyclic voltammetric studies showed two voltage regions of electrochemical activity, one around 4 V and the other above 4.4 V. While the 4-V activity was related solely to the Mn^{4+}/Mn^{3+} couple, the 5-V activity was due to the redox reactions of Ni and the other transition metal ions. The divalent co-substituents did not influence the 4-V capacity. All the co-substituents led to a reduction in the 5-V capacity and to a shifting of the redox potentials in the 5-V region to higher values. The decrease in capacity with an increase in the co-substitutent concentration is related to the increased occupancy of the co-substituents in the 8*a* sites, which can impede the transport of lithium ions during the charge–discharge processes. Among all the compositions studied, $LiNi_{0.4}Fe_{0.1}Mn_{1.5}O_4$ registered the best performance with a first-cycle capacity of 117 mAh/g and capacity retention of 78% over 60 cycles. Electrochemical impedance spectroscopic studies showed a decrease in the charge transfer resistance at high deintercalation levels. To summarize, multiple-substitution is an effective way to improve the operating voltage of the spinel cathode materials based on $LiMn_2O_4$. Although tapping their full capacities over extended cycles may require stable electrolytes, they do represent a class of materials for high energy density lithium batteries.

References

[1] Y. Xia, Y. Zhou, M. Yoshio, J. Electrochem. Soc. 144 (1997) 2593.
[2] R.J. Gummow, A. de Kock, M.M. Thackeray, Solid State Ionics 69 (1994) 59.
[3] G.G. Amatucci, C.N. Schmutz, A. Blyr, C. Sigala, A.S. Gozdz, D. Larcher, J.M. Tarascon, J. Power Sources 69 (1997) 11.
[4] M.M. Thackeray, Y. Shao-Horn, A.J. Kahaian, Electrochem. Soild State Lett. 1 (1996) 160.
[5] A. Yamada, J. Solid State Chem. 122 (1996) 160.
[6] P. Arora, B.N. Popov, R.E. White, J. Electrochem. Soc. 145 (1998) 807.
[7] D.H. Jiang, J.Y. Shin, S.M. Oh, J. Electrochem. Soc. 143 (1996) 2204.
[8] Y. Gao, J.R. Dahn, Solid State Ionics 84 (1996) 33.
[9] J.M. Tarascon, W.R. McKinnon, F. Coowar, T.N. Bowmer, G.G. Amatucci, D. Guyomard, J. Electrochem. Soc. 141 (1994) 1421.
[10] S.T. Myung, H.T. Chung, S. Komaba, N. Kumagai, H.B. Gu, J. Power Sources 90 (2000) 103.
[11] T. Ohzuku, S. Takeda, M. Iwanaga, J. Power Sources 81–82 (1999) 90.
[12] J.H. Lee, J.K. Hong, D.H. Jang, Y.K. Sun, S.M. Oh, J. Power Sources 89 (2000) 7.
[13] T. Ohzuku, K. Ariyoshi, S. Takeda, Y. Sakai, Electrochim. Acta 46 (2001) 2327.
[14] J. Morales, L. Sanchez, J.L. Tirado, J. Solid State Electrochem. 2 (1998) 420.
[15] M.Y. Song, D.S. Ahn, S.G. Kang, S.H. Chang, Solid State Ionics 111 (1998) 237.
[16] Y. Ein-Eli, W.F. Howard Jr., J. Electrochem. Soc. 144 (1997) L205.
[17] Y. Ein-Eli, W.F. Howard, S.H. Lu, S. Mukerjee, J. McBreen, J.T. Vaughey, M.M. Thackeray, J. Electrochem. Soc. 145 (1998) 1238.
[18] Y. Ein-Eli, J.T. Vaughey, M.M. Thackeray, S. Mukerjee, X.Q. Yang, J. McBreen, J. Electrochem. Soc. 146 (1999) 908.
[19] R. Thirunakaran, B. Ramesh Babu, N. Kalaiselvi, P. Periasamy, T. Prem Kumar, N.G. Renganathan, M. Raghavan, N. Muniyandi, Bull. Mater. Sci. 24 (2001) 51.
[20] S.T. Myung, S. Komaba, N. Kumagai, J. Electrochem. Soc. 148 (2001) A482.
[21] F. Le Cras, D. Bloch, M. Anne, P. Strobel, Solid State Ionics 203 (1996) 89.
[22] N. Hayashi, H. Ikuta, M. Wakihara, J. Electrochem. Soc. 146 (1999) 1351.
[23] K. Amine, H. Tukamoto, H. Yasuda, Y. Fujita, J. Electrochem. Soc. 143 (1996) 1607.
[24] Y. Gao, K. Myrtle, M. Zhang, J.N. Reimers, J.R. Dahn, Phys. Rev. B 54 (1996) 3878.
[25] Y. Xia, T. Sakai, T. Fujieda, M. Wada, H. Yoshinaga, Electrochem. Solid State Lett. 4 (2001) A9.
[26] K.A. Striebel, A. Rougier, C.R. Horne, R.P. Reade, E.J. Cairns, J. Electrochem. Soc. 146 (1999) 4339.
[27] H. Kawai, M. Nagata, H. Tukamoto, A.R. West, J. Power Sources 81–82 (1999) 67.
[28] M.M. Thackeray, W.I.F. David, P.G. Bruce, J.B. Goodenough, Mater. Res. Bull. 18 (1983) 461.
[29] M.M. Thackeray, Prog. Solid State Chem. 25 (1997) 1.
[30] C. Sigala, A. Le Gal La Salle, Y. Piffard, D. Guyomard, J. Electrochem. Soc. 148 (2001) A812.
[31] G.T.-K. Fey, C.H. Lu, T. Prem Kumar, Mater. Chem. Phys., in press.
[32] K. Amine, H. Yukamoto, H. Yasuda, Y. Fujita, J. Power Sources 68 (1997) 604.

[33] Y. Shao-Horn, R.L. Middaugh, Solid State Ionics 139 (2001) 13.

[34] Y.I. Jiang, B. Huang, W. Wang, D.R. Sadoway, G. Ceder, Y.M. Chiang, H. Liu, H. Tamura, J. Electrochem. Soc. 146 (1999) 862.

[35] Q. Zheng, A. Bonakdarpour, M. Zhong, Y. Gao, J.R. Dahn, J. Electrochem. Soc. 144 (1997) 205.

[36] J.M. Tarascon, E. Wang, F.K. Shokoohi, W.R. McKinnon, S. Colson, J. Electrochem. Soc. 138 (1991) 2859.

[37] S.T. Myung, S. Komaba, N. Kumagai, J. Electrochem. Soc. 148 (2001) A482.

[38] Y.S. Lee, M. Yoshio, Electrochem. Solid State Lett. 4 (2001) A85.

[39] W.D. Johnston, R.R. Heikes, D. Sestrich, J. Phys. Chem. Solids 7 (1958) 1.

[40] M.D. Levi, G. Salitra, B. Malkovsky, H. Teller, D. Aurbach, U. Heider, L. Heider, J. Electrochem. Soc. 146 (1999) 1279.

[41] D. Aurbach, M.D. Levi, E. Levi, H. Teller, B. Markovsky, G. Salitra, U. Heider, L. Heider, J. Electrochem. Soc. 145 (1998) 3024.

[42] M.D. Levi, K. Gamolsky, D. Aurbach, U. Heider, R. Oesten, Electrochim. Acta 45 (2000) 1781.